引用格式：TIAN Liping, SHEN Lingbin, CHEN Lin, et al. Spatio-temporal Resolution Studies on a Synchronous Streak Tube [J]. Acta Photonica Sinica, 2021, 50(4):0404002
田丽萍,沈令斌,陈琳,等. 同步扫描管时空分辨特性研究[J].光子学报,2021,50(4):0404002

同步扫描管时空分辨特性研究

田丽萍[1],沈令斌[1],陈琳[1],李立立[2],陈萍[2],田进寿[2]
(1 金陵科技学院 网络与通信工程学院,南京 211169)
(2 中国科学院西安光学精密机械研究所 瞬态光学与光子技术国家重点实验室,超快诊断技术重点实验室,西安 710119)

摘 要:设计了一种具有高空间分辨率、高时间分辨率和大工作面积的同步扫描条纹管.建立三维模型,系统地分析了物理时间分辨率与加速电压、空间分辨率与偏转系统-光电阴极的距离、动态空间分辨率和时间分辨率与扫描速度的关系.给出最优化结构参数和电气参数:d_{DC}=100 mm, U_g=700 V, T_{screen}= 0.5 ns.数值模拟结果表明,在光电阴极有效工作面积18 mm×2 mm范围内,静态和动态空间分辨率分别高于25 lp/mm @ MTF=10%和16 lp/mm @ MTF=10%.在T_{screen}=0.5 ns时,同步条纹管的时间分辨率优于5.6 ps.此外,实验测试得到在400 nm波长处,光电阴极的辐射灵敏度为51 mA/W,光电阴极有效面积内的静态空间分辨率高于25 lp/mm @ CTF=13%.

关键词:同步条纹管;物理时间分辨率;空间分辨率;阴极有效面积;全屏时间;阴极灵敏度;调制传递函数
中图分类号:O463 **文献标识码**:A **doi**:10.3788/gzxb20215004.0404002

Spatio-temporal Resolution Studies on a Synchronous Streak Tube

TIAN Liping[1], SHEN Lingbin[1], CHEN Lin[1], LI Lili[2], CHEN Ping[2], TIAN Jinshou[2]
(1 *School of Network and Communication Engineering, Jinling Institute of Technology, Nanjing* 211169, *China*)
(2 *Key Laboratory of Ultra-fast Photoelectric Diagnostics Technology, State Key Laboratory of Transient Optics and Photonics, Xi'an Institute of Optics and Precision Mechanics, Chinese Academy of Sciences, Xi'an* 710119, *China*)

Abstract: A synchronous streak tube capable of providing high spatial resolution, high temporal resolution and large working area is numerically designed and experimentally demonstrated. In this paper, a 3-D model developed to systematically and comprehensively analyze the dependence of the physical temporal resolution on the accelerating voltage, the spatial resolution on the deflector-to-cathode distance, the dynamic spatial resolution and temporal resolution on the scanning velocity. Finally, geometry and electric parameters of d_{DC}=100 mm, U_g=700 V, and T_{screen}= 0.5 ns are proposed to optimize the streak tube performances. The numerical simulations show that the static spatial resolution is higher than 25 lp/mm @ MTF=10% and the dynamic spatial resolution is higher than 16 lp/mm @ MTF=10% over the whole effective photocathode area of 18 mm×2 mm. And, the simulated temporal resolution is better than 5.6 ps

Foundation item: Ph.D. Project Supported by the Jinling Institute of Technology (Nos. jit-b-202012, jit-b-201814), the Natural Science Foundation of Jiangsu Province, China (No. BK20190112), the National Natural Science Fund (No. 12005083), the Scientific Instrument Developing Project of the Chinese Academy of Sciences (No. GJJSTD20190004).
First author: TIAN Liping (1990—), female, lecturer, Ph. D. degree, mainly focuses on electro-optical system design. Email: tianliping@jit.edu.cn.
Corresponding author: TIAN Jinshou (1970—), male, professor, Ph.D. degree, mainly focuses on ultrafast diagnostic technology and photoelectric imaging technology. Email: tianjs@opt.ac.cn
Received: Oct.23,2020; **Accepted**: Feb.14,2021

at T_{screen}=0.5 ns. Furthermore, the photocathode radiant sensitivity can reach 51 mA/W at the wavelength of 400 nm. The tested static spatial resolution is as high as 25 lp/mm @ CTF=13%.

Key words: Synchronous streak tube; Physical temporal resolution; Spatial resolution; Photocathode effective area; Full-screen time; Photocathode radiant sensitivity; Spatial transfer modulation function

OCIS Codes: 040.1880; 230.2090; 230.0250; 170.6920

0 Introduction

The Streak Cameras (SC) can work in two mode which are single-shot mode for strong light signal and synchroscan repetitive mode for weak light signal. In single-shot mode, a ramp voltage applied on the scanning deflector to realize the conversion of high-speed time signal to low-speed space signal. In synchroscan mode, we utilizes a sinusoidal voltage, in synchronism with the laser pulse train and repetition rate of the recorded light pulse, as the scanning voltage applied to the deflection system to realize the diagnosis of the weak repetitive signal[1]. Compared with the single-shot streak camera, the Synchroscan Streak Camera (SSC) providing both high temporal resolution, high sensitivity and high dynamic range is a promising imaging detection system, especially in the measurement of fluorescence lifetime, charge transfer and other fields of applications in which the light signal is very weak[2-4].

At present, several communities have designed and manufactured a number of streak tubes which have excellent performances including high spatial resolution and large effective working area. However, many of them works in single shot mode to achieve strong light diagnosis. In synchroscan mode, the most prominent synchroscan streak camera SC-10 is developed by Optronis in Germany which has achieved the scanning frequency of up to 250 MHz and a time resolution up to 2 ps. However, its spatial resolution is only 5 lp/mm @ 8 mm×2 mm[5]. Otherwise, the synchroscan streak tube Photochron 5 with an accelerator mesh and three focus electrodes developed in Photek has achieved up to 250 MHz scanning frequency and 50 lp/mm spatial resolution. However, its slit effective working length is only 8 mm[6]. The research shows that a high spatial resolution and a large effective working area are a conflict[7]. At present, the most commonly used way to improve the edge spatial resolution is adopted a curved photocathode and a curved screen to decrease the edge space aberrations. An accelerating mesh is often set near the cathode to achieve a high temporal resolution. But, a curved mesh is easily deformed at a high voltage which will cause potential disturbance, thereby reducing the spatial resolution. Although the predecessors have done a lot of research on the streak tube, considerable uncertainties still exist in the estimation of temporal and spatial resolution.

In this paper, a large format, high spatiotemporal resolution and high photocathode sensitivity streak tube (used in the 2200-streak camera of XIOPM) was designed, manufactured and tested. The streak tube consists of a plane photocathode, a plane ultra-fine structure mesh, a focus electrode, a pair of deflection plates, a pair of blanking plates, an anode and a phosphor screen. We adopt a plane mesh electrode to ensure the photoelectrons uniformly focusing through the entire cathode and to accelerate electrons to a high energy in a short distance, thereby improving the temporal resolution. The voltage between photocathode and mesh electrode is a crucial parameter for the streak tube, which has a great impact on the physical temporal resolution. The scanning velocity is also an essential factor for the dynamic spatial resolution. In addition, the dynamic spatial resolution, which shows a significant various trend, decreases with the scanning velocity. The numerical simulation results demonstrate that the static spatial resolution is higher than 25 lp/mm @ MTF=10% in sagittal direction over the whole working area of 18 mm×2 mm. The physical temporal resolution is better than 10 ps and the ultimate physical temporal resolution is about 2 ps. Besides, the static experimental test shows that the spatial resolution is higher than 25 lp/mm @ CTF=13%.

1 Theory and simulation details

The numerical simulations are based on the Finite Integral Technique, Monte Carlo method and 5th order Runge-Kutta method[8-9]. And, the model is built with a commercial software Computer Simulation Technology (CST) STUDIO SUITE. The three-dimensional simulations are carried out in the time-domain, that including the tracking and the particle in cells solvers which will study the streak tube in a numerical way.

Fig.1 exhibits the streak tube model which components of a photocathode, an accelerating mesh, a focus system, a pair of deflection and blanking plates, anode and a phosphor screen. The incident ultrafast light pulse is first converted by the photocathode to an ultrafast electron pulse, correspondingly. Thus, the ultrafast electron pulses can be regarded as the replica of the light pulse. Then, the ultrafast electron pulse will be accelerated by the strong electrostatic field between the photocathode and the mesh electrode, and focused by the focus electrode, respectively. Furthermore, with the scanning signal on the deflection scanning system, the electron pulses can achieve time-to-space transformation[1]. At last, the reshaped electron pulse is converted to an optical image on the phosphor screen. It is a remarkable fact that the output of the light intensity on the screen is proportional to the number of photoelectrons generated by the photocathode, which is in proportion to the incident light intensity. In the model, all electrodes are replaced by the Perfect Electric Conductors (PECs) and the phosphor screen is replaced by vacuum material, and a 2D electronic position monitor can be set on its surface to statistics of electron position dispersion information. The electric field in the streak tube calculated at an operating voltage of -7.6 kV is exported for further beam characteristic evaluation. It is worth noting that the extraction field between the accelerating mesh and the cathode is 470 V/mm. The streak tube is a rotationally symmetric structure while it works in static mode. The scanning deflection plates is set in the equipotential zone.

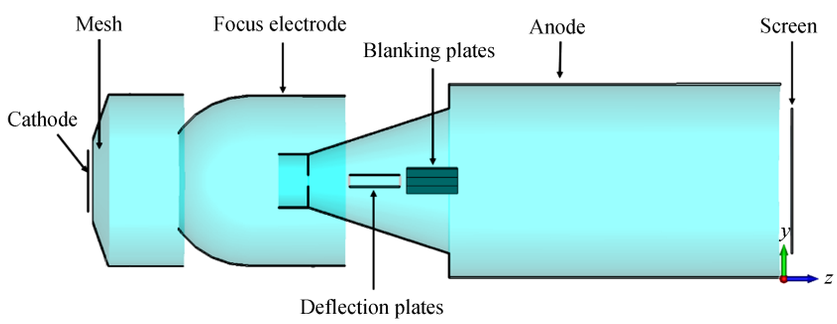

Fig.1 Streak tube model and electric field density distribution along z-axis

The electrons emitted from the photocathode are not random and disorderly while the photocathode is illuminated by light. Some research and experiments suggest that the much more precise model of photoelectron emitted from the photocathode should be the Monte-Carlo sampling simulation with following considerations[10-11]. 1) The energy of emitted photoelectrons has a (0~0.6 eV) $\beta(1,4)$ distribution and the most probable energy of electrons is 0.15 eV; 2) The inclination of emitted photoelectrons has a cosine distribution in a range of 0 to $\pi/2$, which is fairly independent of the initial incident energy; 3) The azimuth of emitted photoelectrons has evenly distribution from 0 to 2π, which is fairly independent of the initial energy and inclination; 4) The position of the photoelectrons has an uniform distribution, which is independent of the initial incident energy, inclination and azimuth. It is noteworthy that the four parameters above are fully uncorrelated from each other. Otherwise, since the spatial resolution of the screen is generally higher than 100 lp/mm which is much higher than that of electro-optical system. Therefore, in the calculation of spatial resolution, only the position dispersion of photoelectrons at the screen is considered.

2 Results and discussions

2.1 Static characteristics of spatiotemporal resolution

The physical temporal resolution and spatial resolution in static mode is thoroughly investigated. To study the physical temporal resolution of our ST, we simulated the relationship between the physical temporal resolution and the off-axis distance (x) for different voltages applied between the photocathode and the accelerating electrode (U_g). The results show that the physical temporal resolution is a function of the U_g and x, as shown in Fig. 2 (a). The increasing U_g improves the physical temporal resolution, because the higher accelerating voltage shortens the transit time of photoelectrons in the streak tube, which in turn shortens the transit time dispersion of the photoelectrons. Furthermore, with the increasing of x, the physical temporal

resolution gradually deteriorates, because the edge field effect of the electric lens will lead different force between electron bunches emitted from different off-axis distances and center of the cathode. Also, the path differences of the photoelectrons is greater on edge of the effective working area than in the center of the cathode. Moreover, the temporal resolution over the whole effective photocathode of the streak tube is in the range of 1～14 ps. From previous research[12] which demonstrate that the spatial resolution will deteriorate with the increasing accelerating voltage U_g. In this paper, U_g=700 V is employed. Fig. 2(b) gives the ultimate physical Temporal Modulation Transfer Function (TMTF) which shows that the ultimate physical temporal resolution is 4.4 ps on axis.

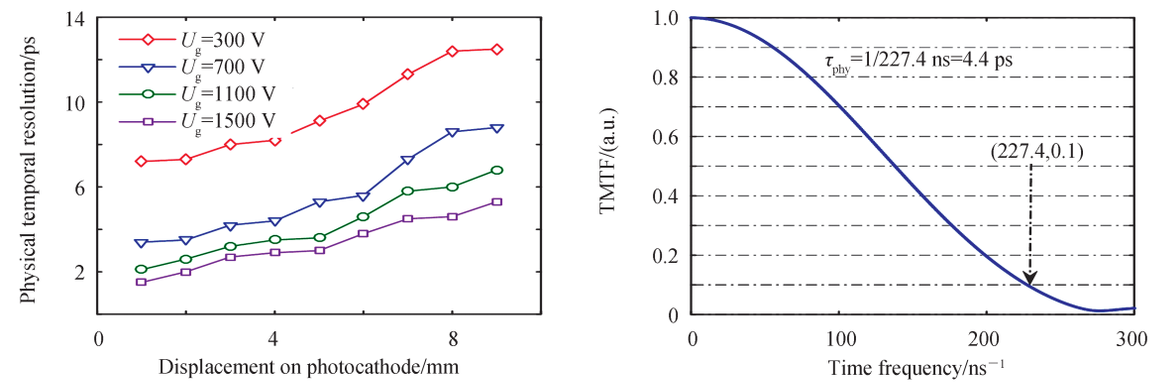

(a) Physical temporal resolution versus different x and U_g (b) Ultimate physical temporal modulation transfer function while U_g=700 V

Fig.2 Physical temporal resolution

The electron beam emitted at the cathode center is only affected by the spherical aberration, while the off-axis points are affected by several aberrations including distortion, coma and field curvature aberrations at the same time. Thus, the further away from the axis, the lower the spatial resolution is. Fig. 3 describes the simulated static Spatial Modulation Transfer Function (SMTF) in sagittal direction while U_g=700 V. Obviously, it shows a significant tendency while the off-axis distance is increasing, the static spatial resolution is gradually decreasing. It is worth noting that the spatial resolution is higher than 25 lp/mm even though the off-axis distance is 9 mm.

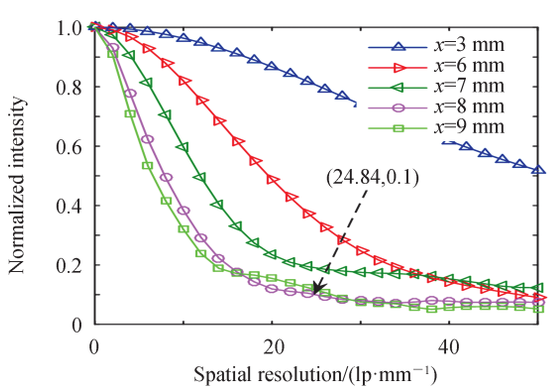

Fig.3 Static SMTF in sagittal direction

2.2 Dependence of dynamic spatial resolution on the deflector position

Electron beams emitted from the cathode have time dispersion due to different initial energy and azimuth. Therefore, the electron beams will first disperse, and then focus into a point at the screen. Significantly, the electron beam diameter decreases gradually when it runs to the entrance of the deflectors. The theoretical study shows that reducing the diameter of the electron beam spot at the entrance of the deflector can reduce the deflection defocusing[13], thereby improving the dynamic spatial resolution. Fig. 4 describes the simulated Dynamic Spatial Modulation Transfer Function (DSMTF) for different distances between deflectors to cathode (d_{DC}) in the range of 85～105 mm. Obviously, with the increasing d_{DC}, the dynamic spatial resolution of the

photocathode center increases until its maximum higher than 100 lp/mm at d_{DC} =100 mm and then decreases. Thus, to obtain a high spatial resolution, the deflectors are set 100 mm away from the photocathode.

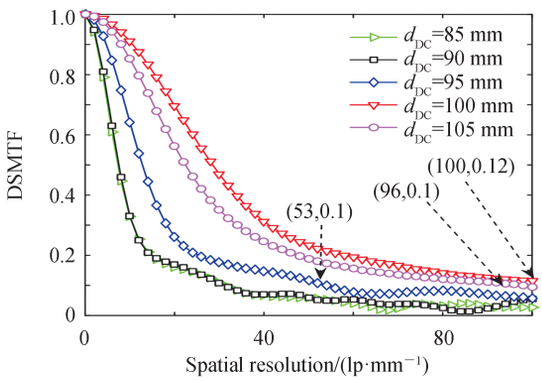

Fig.4 DSMTF of the ST at different d_{DC}

2.3 Dependence of dynamic spatial resolution on the scanning velocity

Fig. 5 describes the simulated dynamic spatial resolution variation for different full screen scanning time (T_{screen}) ranging from 0.8 to 0.36 ns and different off-axis distance (x) in the interval of 0~8 mm. Simulation results show a pronounced tendency toward spatial resolution versus T_{screen} and x behavior. The increasing T_{screen} decreases the scanning velocity and deflection defocusing, thereby improving the spatial resolution. When the off-axis distance increases, the aberrations will increase, resulting in a large spatial dispersion of the photoelectrons, which will reduce the spatial resolution.

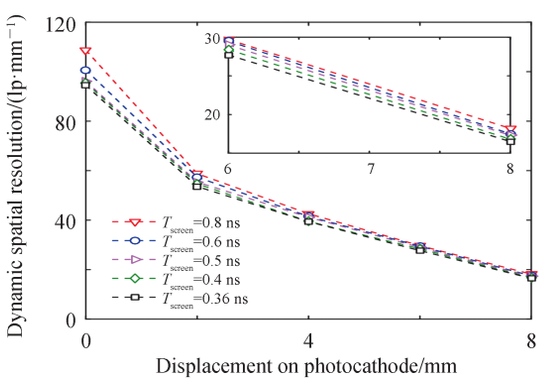

Fig.5 Dynamic spatial resolution of the ST versus scanning frequency

The greater the scanning deflection distance of the electron bunches at the screen, the lower dynamic spatial resolution is. It is because that the electron bunches have a large space dispersion at the operation of fast-speed scanning. In this paper, an appropriate scanning point is selected so that the electron beams deviate from the center of the screen about 12 mm to achieve a better spatial resolution. Fig. 6 shows the dynamic spatial modulation transfer function at different point of cathode along sagittal direction at T_{screen}=0.5 ns. It is obvious that the dynamic spatial resolution gradually decreases with the increasing of the off-axis distance, and the dynamic spatial resolution is higher than 16 lp/mm over the whole effective cathode working length of 18 mm.

2.4 Temporal resolution on scanning mode

The temporal resolution is defined as the Full Width at Half Maximum (FWHM) of the intensity of the streak image on the screen while the temporal width of the incident light pulse can be almost neglected. It comes mainly from the Transit Time Spread (TTS) of the electrons initial angle dispersion, and the space dispersion caused by deflector scanning. In this paper, two electron bunches with an interval of 20 ps and FWHM of 100 fs are emitted from the inner surface of the cathode, as shown in Fig.7 (a). The scanning signal, shown in Fig.7 (b), is applied on the deflectors with amplitude of 750 V. To reduce the photon electrons spatial distortion

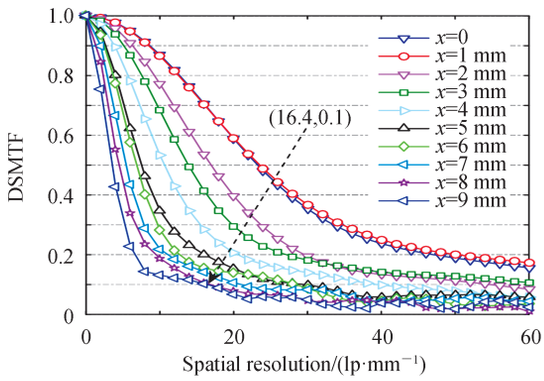

Fig.6 DSMTF of the ST along x direction

produced by the scanning signal and improve the dynamic spatial resolution, we synchronize the electron beam in the range of quasi-linear area of the scanning signal. The scanning electron image is as shown in Fig.8. Two electron beams can be completely separated according to the Rayleigh Criterion and the FWHM of the scanning electrons on phosphor screen is only 5.6 ps. Thus, the temporal resolution of the ST is better than 5.6 ps @ T_{screen}=0.5 ns.

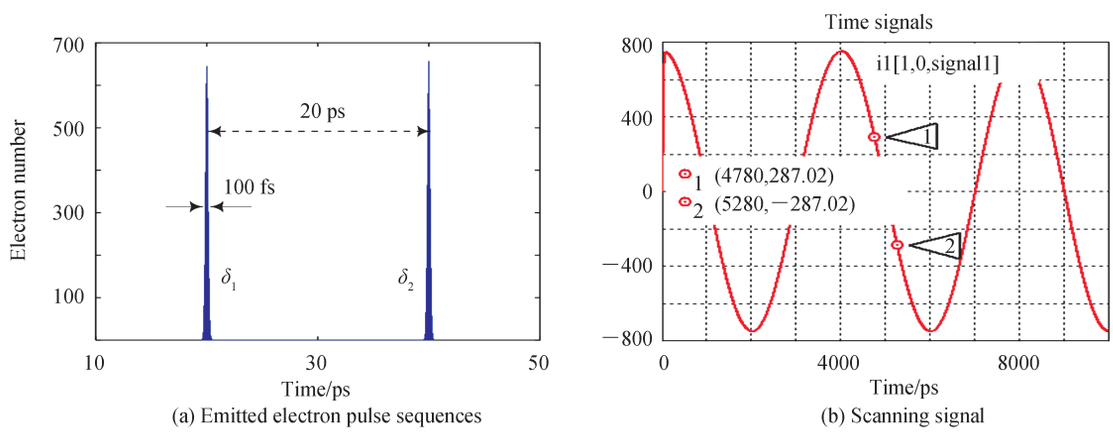

Fig.7 M-C sampling electron pulse sequences and synchronous scan signal

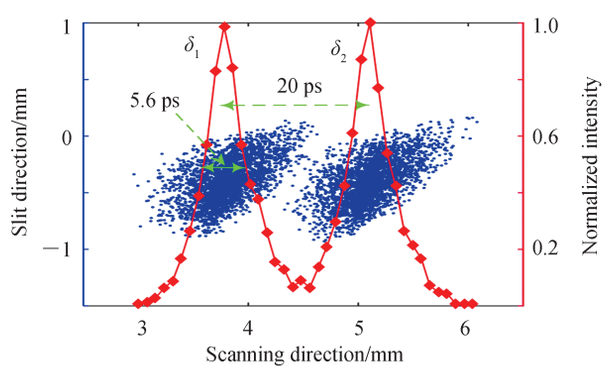

Fig.8 Sweeping results of electron pulses with a duration of 20 ps

The dependence of the temporal resolution on T_{screen} is thoroughly investigated in a numerical way. In this paper, T_{screen} is varied from 0.8 to 0.36 ns, and the values of scanning voltage amplitude are fixed at ±750 V. Simulation result shows a pronounced linearity tendency in Fig.9. The decreasing T_{screen} improves the temporal resolution due to the scanning velocity increasement, thereby increasing the deflection distance of photoelectron along the scanning direction during the same transit time. It can also be explained by a formula for temporal resolution which expressed as[15].

$$\begin{cases} \tau = \sqrt{\left(\dfrac{m \cdot \Delta v_e}{4eE}\right)^2 + \left(\dfrac{\mu}{4v}\right)^2} \\ v = \dfrac{H_{\text{screen}}}{T_{\text{screen}}} \end{cases} \tag{1}$$

where e and m are the electron charge and mass. E, $\Delta v_e$are the electric field near the photocathode and half of amplitude width of the initial energy. v and μ are the scanning velocity and dynamic spatial resolution in meridian direction, H_{screen} is the effective phosphor screen which is fixed. With the decrease of scanning velocity, the spatial resolution will increase while the space dispersion will decrease due to a small deflection distance at the screen. Obviously, the temporal resolution will deteriorate approximately linearly with the increase of T_{screen}.

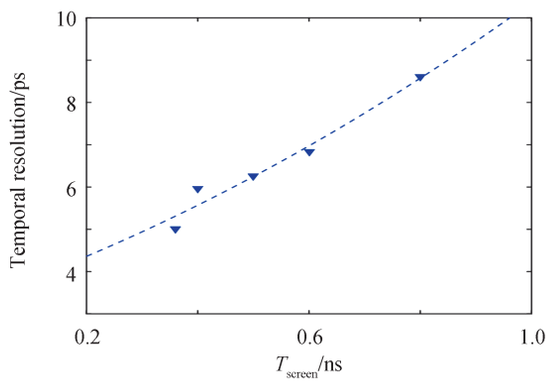

Fig.9 Temporal resolution versus scanning velocity

3 Performances in 2200-synchroscan streak camera

Based on the previous theoretical electro-optical design, we have successfully manufactured a prototype of the streak tube with metal-ceramic-glass package, which is shown in Fig.10. The streak tube is potted with high magnetic permeability and high conductivity materials for packaging, which can improve its anti-electromagnetic interference ability. The internal surface of the ceramic is deposited with Cr_2O_3, which would have great contribution in avoiding the electric breakdown. A S-20 photocathode and P-43 phosphor screen are employed to response visible light and to obtain a high electron-optical conversion efficiency. We test the initial performance of the tube including Photocathode Radiant Sensitivity (PRS) and Modulation Transfer Function (MTF) in the STR test station, detailed description seen in the articles[9-10]. A schematic diagram of PRS, MTF and spatial resolution test is shown as Fig.11.

Fig.10 The manufactured ST

The TAL light source is an electronically controlled LED plane light source , including LED light source at wavelength of 590 nm and 2 850 K color temperature polychromatic source, which can be used to test the spatial resolution and MTF. The BAL light source is integrated with ARW rotary wheel with a set of spectral filters, which can be adopted to test the PRS of the streak tube. The UNI is a camera of wide field of view with

unit magnification, and the MR2 is an imaging radiometer of narrow field of view with magnification of 100, which can be used to resolved the details of the streak tube imaging.

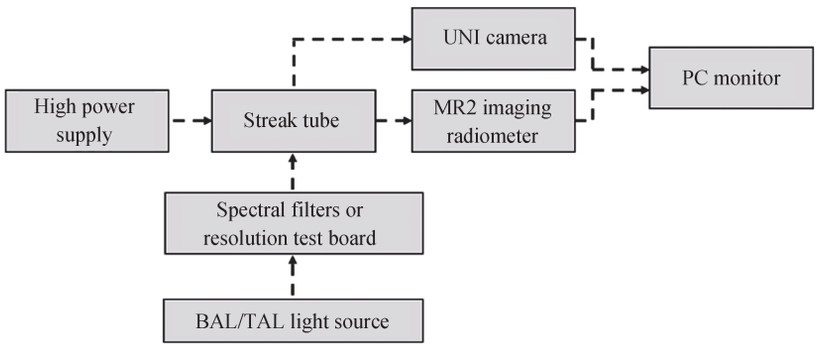

Fig.11 Schematic diagram of PRS, MTF and spatial resolution test

3.1 Photocathode radiant sensitivity of the ST

Photocathode Radiant Sensitivity (PRS) of the streak tube is measured as ratio of photocathode current (mA) to incoming radiation power (W) at a specified wavelength, which is typically measured in mA/W. In the experiment, BAL light source with the power density of the photocathode irradiation light signal of 1 mW/m^2 is irradiated on the photocathode after passing through a set of spectral filters from at least 400 nm to 850 nm. Otherwise, the optical aperture with Φ16 mm is set before the photocathode to improve the test precision by avoiding the non-uniformity light. And, a constant DC acceleration voltage of +200 V is applied between the cathode and the mesh electrode which is almost response to a saturated photocurrent. As shown in Fig.12, the maximum value of PRS reaches 51 mA/W at the wavelength of 400 nm, which will provide a good performance for a visible imaging system.

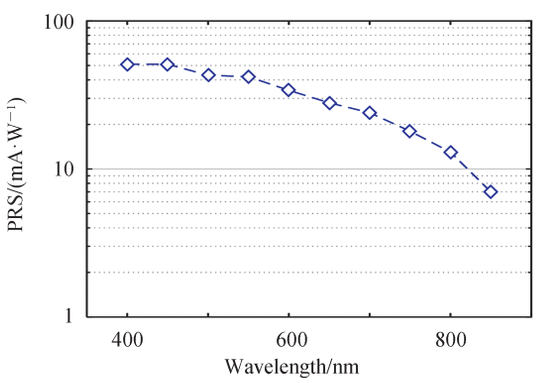

Fig.12 PRS of the streak tube

3.2 Static spatial resolution of the streak tube

In the spatial resolution test, we adopt the spatial modulation transfer function to evaluate the spatial resolution of the cathode center, and the resolution target method to evaluate it of the edge. In the experiment, a continuous optical signal with a central wavelength of 590 nm and a strength of 10 lx is used to irradiate photocathode to obtain the SMTF of the ST, as shown in Fig. 13(a). It is evident that the central spatial resolution on the photocathode is higher than 35 lp/mm. We also test the spatial resolution of the edge in which the resolution target board is employed. It contains different resolutions of patterns in four directions. The test image result is shown as Fig. 13(b). A resolution pattern image with 25 lp/mm is selected for analysis. The intensity distribution curve of the selected part in the insert image is shown as Fig. 13(b). According to the Rayleigh criterion, we can conclude that the edge spatial resolution is higher than 25 lp/mm@ CTF=13%.

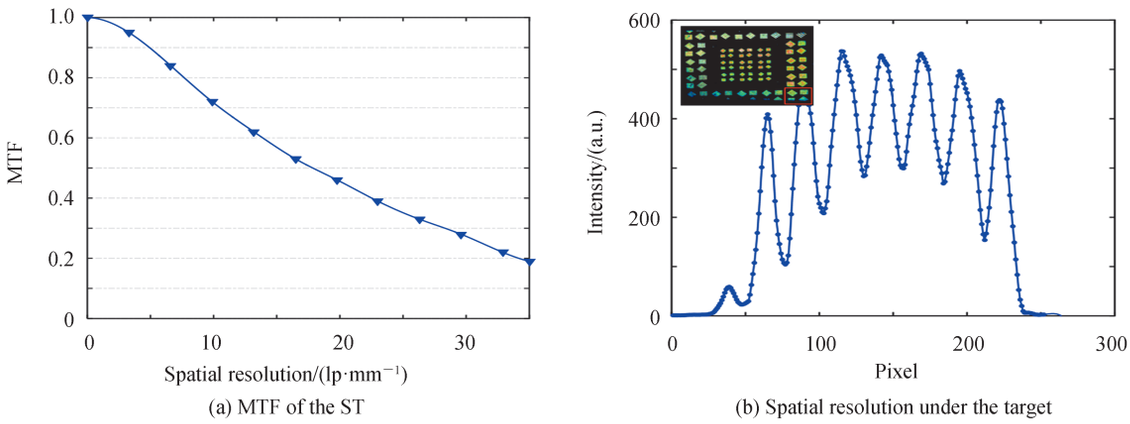

Fig.13 Measured static spatial performance of ST

3.3 Comparison of experimental and simulation results

In Fig.14, the blue curve is the experimental SMTF of the streak tube which shows the spatial resolution is 35 lp/mm @ MTF=19%, while the red curve is the theoretical of it which shows the spatial resolution is 35 lp/mm @ MTF=69%. Obviously, the experimental spatial resolution characteristic is lower than the theoretical value, which may be caused by the following reasons: 1) In the theoretical calculation, we did not consider the lateral dispersion effect of the electron spot caused by the space charge effect, which would deteriorate the spatial resolution; 2) In the experiment, we did not consider the coupling efficiency of MR2 and the streak tube. And, the assembly error of the streak tube will also affect the distribution of the electromagnetic field, thus reducing the spatial resolution.

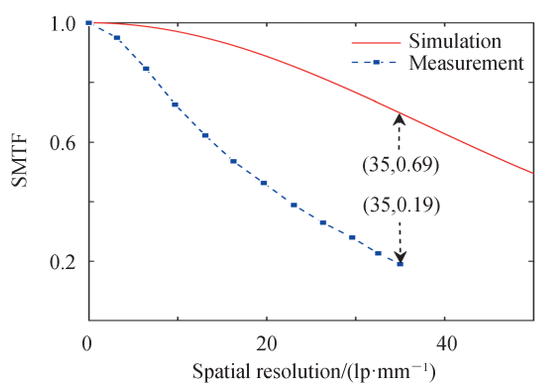

Fig.14 SMTF comparison of experimental and simulation

4 Conclusion

We successfully demonstrate a synchronous streak tube with high spatiotemporal resolution over the whole working area of 18 mm×2 mm. The analyzations reveal that temporal resolution will improve with the increase of the field between the photocathode and the mesh. Moreover, when the scanning speed is increasing, the spatial resolution would increase, while the temporal resolution decreases. And also, there is best distance between the deflection plate and the photocathode which is of 100 mm, makes the better spatial resolution. The simulation results show that the static spatial resolution is higher than 25 lp/mm @ MTF=10%. While T_{screen} is 0.5 ns, the dynamic spatial resolution is higher than 16 lp/mm @ MTF=10% and the temporal resolution is better than 5.6 ps. The experiment results show that the MTF of the streak tube is 35 lp/mm @ MTF=19% in the center of the photocathode and the static spatial resolution is 25 lp/mm @ CTF=13%. The PRS of the photocathode can reach 51 mA/W @ 400 nm.

References

[1] FINCH A, SLEAT W E, SIBBETT W. Subpicosecond synchroscan operation of a photochron IV streak camera[J].

Review of Scientific Instruments, 1989, 60(5): 839-844.
[2] TAYLOR J R, ADAMS M C, SIBBETT W. Investigation of viscosity dependent fluorescence lifetime using a synchronously operated picosecond streak camera[J]. Applied Physics, 1980, 21(1): 13-17.
[3] KINOSHITA K, INAGAKI Y, ISHIHARA Y, et al. Femtosecond synchroscan streak tube[J]. Japanese Journal of Applied Physics, 2002, 41(1): 389-392.
[4] ADAMS M C, SIBBETT W, BRADLEY D J. Linear picosecond electron-optical chronoscopy at a repetition rate of 140 MHz[J]. Optics Communications, 1978, 26(2): 273-276.
[5] TSIKOURAS A, NING J, NG S, et al. Streak camera crosstalk reduction using a multiple delay optical fiber bundle[J]. Optics Letters, 2012, 37(2):250-252.
[6] Online Computer Library Center, Inc. Photochron 5 datasheet[EB/OL]. [2017-04-03]. http://www.photek.co.uk/products/datasheets.html.
[7] XIA W, HAN S, ULLAH N, et al. Design and modeling of three-dimensional laser imaging system based on streak tube[J]. Applied Optics, 2017, 56(3): 487-497.
[8] TIAN Liping, TIAN Jinshou, WEN Wenlong, et al. Electro-optical design of a long slit streak tube[C]. SPIE, 2017.
[9] HUI Dandan, LUO Duan, TIAN Liping, et al. A compact large-format streak tube for imaging lidar[J]. Review of Entific Instruments, 2018, 89(4): 045113.
[10] TIAN Liping, LI Lili, WEN Wenlong, et al. Numerical calculation and experimental study on the small-size streak tube[J]. Acta Physica Sinica, 2018, 67(18): 188501.
[11] HUI Dandan, TIAN Jinshou, LU Yu, et al. Temporal distortion analysis of the streak tube[J]. Acta Physica Sinica, 2016, 65(15): 158502.
[12] Online Computer Library Center, Inc. ST-X datasheet[EB/OL]. http://www.photek.co.uk/pdf/datasheets/detectors/DS028-ST-X-Streak-Tube-Datasheet.pdf.
[13] HUA Z Y, GU C X. Electron optics[M]. Shanghai: Fudan University Press, 1993: 237-246.
[14] BAD'IN L V, DEMIN S K, SAFRONOV S I, et al. Computer-aided designing of simple electron-optical systems for electron image tubes[J]. Technical Physics, 2011, 56(8): 1167-1174.